Heteroepitaxial Growth and Surface Structure of $L1_0$-MnGa(111) Ultra-thin Films on GaN(0001)

Andrada-Oana Mandru[1], Reyes Garcia Diaz[1,2], Kangkang Wang[1*], Kevin Cooper[1], Muhammad Haider[1,3], David C. Ingram[1], Noboru Takeuchi[1,2], and Arthur R. Smith[1†]

[1]*Nanoscale and Quantum Phenomena Institute, Department of Physics and Astronomy, Ohio University, Athens, OH 45701, USA*

[2]*Centro de Nanociencias y Nanotecnologia, Universidad Nacional Autónoma de México, Apartado Postal 14, Ensenada Baja California, Codigo Postal 22800, México and*

[3]*Department of Physics, King Fahd University of Petroleum and Minerals, Dhahran, 31261, Saudi Arabia*

Abstract

$L1_0$-structured MnGa(111) ultra-thin films were heteroepitaxially grown on GaN(0001) under lightly Mn-rich conditions using molecular beam epitaxy. Room-temperature scanning tunneling microscopy investigations reveal smooth terraces and angular step edges, with the surface structure consisting primarily of a 2×2 reconstruction along with small patches of 1×2. Theoretical calculations were carried out using density functional theory, and the simulated STM images were calculated using the Tersoff-Hamman approximation, revealing that a stoichiometric 1×2 and a Mn-rich 2×2 surface structure give the best agreement with the observed experimental images.

Keywords: manganese gallium; scanning tunneling microscopy; molecular beam epitaxy; density functional theory

PACS: 68.35.-p; 68.37.Ef; 75.70.-i; 71.15.Mb

* new address: Recording Media Operations, Seagate Technology, Fremont, CA 94538

† corresponding author, e-mail: smitha2@ohio.edu

Manganese gallium (MnGa) alloys have been a subject of interest recently due to their advantageous properties such as high spin polarization, low damping terms, and large coercivity.[1–3] The magnetic properties of this system are known to be highly dependent on the Mn:Ga stoichiometry, but also on the choice of substrate onto which the films are deposited.[4] Heusler alloys, of which MnGa is one member, form an important class of magnetic materials.[5, 6] A recent paper has reported a study of how structural, electronic and magnetic properties change with stoichiometry for MnGa layers grown by molecular beam epitaxy (MBE) on GaN(0001).[7] The MnGa/GaN bilayer system is very promising due to the wide interest in developing nitride spintronic systems and because of the observed ideal lattice matching and sharp growth interface.[8]

The focus of this Letter is to present detailed results concerning the surface structure of $L1_0$-structured MnGa ultra-thin films grown on GaN(0001) using scanning tunneling microscopy (STM), since it is widely known that surface structures during MBE growth play an important role in resultant film properties.[9] In particular, it is an important open question as to exactly how the 1×2 and 2×2 reconstructions seen in reflection high energy electron diffraction (RHEED) play a role in determining the magnetic (and also electronic) properties. In other words, it is well-known that as Mn flux increases, the bulk film magnetic properties change;[7, 8] therefore, we want to understand how Mn atoms incorporate into the surface structure which in turn may tell us how they incorporate into the bulk film.

Manganese gallium samples grown under epitaxially smooth and lightly Mn-rich growth conditions are investigated using STM, and the results for both 1×2 and 2×2 structures are compared to structural models and simulated STM images from theoretical calculations. Energies of various models are presented in order to further establish the identification of the locations of the individual atomic species within the two reconstructions.

The custom-designed system in which the sample growth was performed consists of an ultra high vacuum (UHV) MBE chamber equipped with Mn and Ga effusion cells, a radio-frequency nitrogen plasma source, a RHEED system (for growth monitoring), and a quartz crystal sensor (for source flux calibration). The ultra-thin MnGa films were heteroepitaxially deposited on commercially available metal-organic chemical vapor deposition (MOCVD) grown GaN(0001) substrates. Once solvent cleaned, the GaN(0001) substrate is introduced into the MBE chamber and annealed for 30 min at 650°C. Then, a layer of about 100 nm of GaN is grown at a substrate temperature of $\approx$ 700°C. Once the GaN growth ceases, the

substrate temperature is reduced to $\approx$ 250°C and MnGa(111) ultra-thin films ($\approx$ 23 nm in height) are deposited while maintaining the Mn to Ga flux ratio at about 1.09. The freshly grown sample is transferred *in-situ* to the adjacent UHV analysis chamber for room-temperature STM and AES studies. After removal from the vacuum chamber, Rutherford backscattering spectrometry (RBS) measurements are performed in order to establish the film stoichiometry.

Calculations are carried out using spin polarized density functional theory as is implemented in the plane waves-self-consistent field code from Quantum ESPRESSO.[10] The Exchange-Correlation functional is treated within the Generalized Gradient Approximation with the Perdew-Burke-Ernzerhof parametrization.[11] The electron-ion interaction is calculated using ultra-soft pseudo-potentials.[12] The energy cutoff used is 30 Ry. Bulk parameters (a and c) are optimized for the ferromagnetic case, which is found to have the lowest energy. For the surface energy calculations, the super-cell approximation is used in which a slab with an artificial periodicity along the z direction is created. Each slab consists of seven atomic (111) layers with four atoms per layer and a 2×2 in plane periodicity. Each of the inner five layers contains two Ga and two Mn atoms, corresponding to two 1×2 ideal bulk MnGa(111) unit cells. The bottom and top most layers have a variable number of Ga and Mn atoms, according to the calculated geometry. A vacuum space of more than 10 Å is used between slabs in order to avoid interactions. Simulations of STM images are obtained by using the Tersoff-Hamman approximation.[13]

Figure 1(a) shows a 3D-rendered, atomic-row-resolved STM image of an atomically smooth (111) surface of an ultra-thin MnGa film grown as described above, acquired at a bias voltage V_s= -11.0 mV and tunneling current I_t= 279 pA. Clear abrupt atomic steps and smooth terraces are characteristic of the surface. The step height is measured to be $\sim$ 2.2 Å, exactly consistent with known experimental lattice constants[7, 8] as well as values based on theoretical calculation, assuming that the surface normal is [111]. The row-row spacing is measured to be $\sim$ 4.6 Å, which is equal to twice the primitive atomic row spacing in the (111) plane for MnGa along $[11\bar{2}]$.

The fact that atomic rows run parallel to some step edges and at $\sim 60^\circ$ to other step edges is more clearly seen in the plan-view STM image presented in Fig. 1(b). There, we see that the row structure is closely linked to the step edge structure. We also notice that the atomic rows on adjacent terraces typically run in the same direction. However, this is

not always the case, as can be seen inside the black boxed regions in Fig. 1(b); zoom-ins of those regions are shown in Figs. 1(c) and 1(d) where the atomic rows in some areas run at $\sim 60^\circ$ or 120° to nearby areas, suggesting the existence of rotated crystalline domains. Also noted is a screw dislocation as seen clearly in Fig. 1(c), having a Burgers vector of B = 2.2 Å along [111]. The approximately 60° rotated domains can be explained by the fact that a stoichiometric MnGa film has only 2-fold symmetry about [111] while the GaN substrate has 3-fold symmetry about [0001]. Thus, the formation of three rotated domains naturally occurs during heteroepitaxy as nucleation takes place.

Thus we have the peculiar situation that although the row-like structure of the surface indicates 2-fold symmetry, the predilection of the surface for forming steps edges at 60° and 120° to each other reveals the nearly hexagonal (hexagon-like) nature of the (111) MnGa surface, consistent with the well-known film-substrate epitaxial lattice matching as found by RHEED.[8] The fact is that MnGa is a face-centered tetragonal crystal, not a perfect cube; but the STM images reveal that atomic diffusion and surface step energetics favor the formation of step edges running along $[1\bar{1}0]$, $[01\bar{1}]$, and $[10\bar{1}]$ (i.e. hexagon-like surface directions), as indicated in Fig. 1(b).

With a very sharp STM tip, row-like regions such as that shown in 1(b) can be atomically resolved into a hexagonal-like 2×2 structure, as shown in 2(a). As clear from this figure, the 2×2 is very well ordered, appearing as a protrusion-type structure. This structure is believed to form under Mn-rich conditions and is observed as a 2×2 RHEED pattern while growing the film. It was proposed by Lu *et al.* that excessive Mn at the surface could result in a periodic substitution of Mn into Ga sites, leading to a 2×2 substitutional model as shown in Fig. 2(d).[8] As shown in Fig. 2(b), the line section measurement along $[1\bar{1}0]$ reveals a periodicity of $\sim$ 5.4 Å, agreeing very well with twice the Mn-Ga interatomic spacing, corresponding to 2×, as seen in the model of Fig. 2(d). Along $[11\bar{2}]$, the line section shows a high peak - low peak profile where the spacing between high peaks is $\sim$ 9.2 Å and the spacing between high and low peaks is $\sim$ 4.6 Å, the inter-row spacing [see Fig. 2(c)]. The low peak corresponds to the saddle point between neighboring bright peaks in the STM image.

Comparing the 2×2 line profiles to the substitutional model, it appears that the Ga atoms protrude more than the Mn atoms in the STM image. Since clearly it is important to evaluate the substitutional 2×2 model theoretically, we have carried out first-principles calculations

to determine which atoms in a substitutional model as shown in Fig. 2(d) dominate the local density of states (LDOS) and as well the formation energy of this model in comparison to energies of competing 2×2 models such as adatom models. Lattice parameters a and c were also calculated for the bulk $L1_0$ ferromagnetic structure and they were found to be 3.83 Å and 3.72 Å, respectively. These values are in good agreement with previous experimental measurements.[4, 7, 14]

Shown in Fig. 3 is a plot of surface formation (total) energy for various structural models considered for the cases of 1×2 and 2×2 structures observed in the STM images. The models include ideal (1Ga 1Mn), vacancy (1Ga, 1Mn), adatom (Ga, Mn), and substitutional (3Ga 1Mn, 1Ga 3Mn), and as can be seen, the substitutional and ideal models are found to be lowest in energy within separate ranges of the chemical potential considered. In particular, the 1Ga 3Mn model is lowest in energy over the Mn-rich regime, followed by the ideal model within an intermediate regime, followed by the 3Ga 1Mn model over the Ga-rich regime. The fact that either ideal or simple substitutional models are preferred is consistent with experimental observations, both in STM and in MBE growth, of either 1× or 2× structures in the vicinity of the stoichiometric flux ratio, allowing a smooth variation of film stoichiometries to be obtained. In subsequent comparisons between experiment and theory, STM simulations are only done for the ideal and substitutional models, namely the ideal 1Ga 1Mn 1×2 and the substitutional 1Ga 3Mn 2×2.

Referring now to Fig. 4, a direct comparison is made between the 2×2 from the experiment and the 2×2 from the theoretical calculation. Presented in Fig. 4(a) is the simulated STM image at distance of 3.0 Å above the surface and corresponding to the experimental STM image V_s of -12.3 mV; I_t for the experimental STM image is 402 pA. The 3.0 Å distance is comparable to a very small tip-sample spacing in STM but is reasonable if not a little on the high side for STM simulations. Overlaid onto the simulated image is the 2×2 substitutional model showing registry between the simulation and the atomic positions of the model. These then are to be compared to the actual STM image with similar model overlay, as shown in Fig. 4(b).

As seen, the agreement between theory and experiment is very good. Bright features in the STM image are reproduced in the simulation at 2×2 symmetry positions. The positions of the bright features correspond to the Ga sites. The Mn atoms protrude less than the Ga atoms, and this is observed in both simulated and actual STM images. Calculations

involving different orbitals around the Fermi level indicate that the Mn atoms dominate the LDOS, in agreement with previous results [15]; however, the LDOS of each Mn is very localized around the atom. Theoretically, since the two Mn atoms in the Mn row [see Fig. 4(a)] are lower than the Mn and Ga (which are at the same height) in the Mn-Ga row by 0.15 Å, and due to the delocalized nature of the Ga atom density, the Ga atom appears brighter. Note that these calculated atomic height differences are not to be compared to the STM corrugations.

From MBE RHEED measurements, a 1×2 is also commonly seen, and as well this is found in the STM images. Shown in Fig. 5(a) is a region of the same sample containing both the 2×2 (lower left corner) and the 1×2 (directly adjacent), and as well a third type of reconstruction shown in the middle to upper right corner of the image which has a symmetry of 2×3. This third structure is much less common on the studied sample but most likely corresponds to a region with slightly higher (or possibly, lower) Mn concentration. The two domains of the 2×3 reconstruction look similar but actually have slightly different structure, intersecting at $\sim 90^\circ$, corresponding to the surface azimuthal directions $[1\bar{1}0]$ and $[11\bar{2}]$.

To verify the 2×2 and 1×2 spacings, line sections are shown in Fig. 5(b). There one sees that the corrugation spacing along $[1\bar{1}0]$ for the 2×2 is exactly 2 times the spacing of the 1×2, as expected, which is also clear from the image.

It may be seen that the 1×2 region is actually a small domain on the surface, surprising given that the Mn:Ga flux ratio was so close to 1:1. Nonetheless, we can directly compare the experimental STM image of the 1×2 with the 1×2 simulation based on theoretical calculations, and this is done in Figs. 5(c) and 5(d). Together with the model overlays, theory and experiment are found to agree very well with each other, with the bright features in the STM image corresponding to the Ga sites in the model.

Despite very good agreement between the STM images and theoretical simulations, an important question comes up since we see in the experiment that only very little of the surface has the stoichiometric 1×2 structure. A relatively large fraction of the surface corresponds to the 3:1 Mn:Ga ratio. This is very interesting since the intended Mn:Ga flux ration was only 1.09. Based on that, one would expect to find most of the surface having the stoichiometric 1×2 structure and only very little of the 2×2 Mn-rich structure. Therefore, we carried out RBS measurements on the same sample, and based on those measurements we find that the 23 nm thick film has a Mn:Ga composition ratio of 0.99 ± 0.05, thus giving a 60% (40%)

confidence that the bulk sample is Ga-rich (Mn-rich). Moreover, we can say with almost 100% confidence that the bulk film has stoichiometry less than the intended 1.09. These RBS numbers are unlikely to be affected by film roughness since the rms roughness is very small, only 0.4 nm.

An estimate of the overall surface composition based on sampling of STM images resulted in a weighted average Mn:Ga ratio of 3.0 ± 0.1. This value was obtained by considering that the 2×2 reconstruction (with Mn:Ga ratio of 3:1) represents ∼ 80% of the surface, the 1×2 (with Mn:Ga ratio of 1:1) ∼ 2%, and the 2×3 (with Mn:Ga ratio ranging from 2:1 to 4:1, since we do not know the exact proportions) the remaining ∼ 18%. To further verify the surface composition of the film, we carried out AES measurements, finding a Mn:Ga ratio of 1.4 ± 0.1 after correcting the Mn and Ga derivative spectra for sensitivity factors. Of course, we would not expect a number larger than this since AES is also sensitive to the underlying stoichiometric layers. A rough prediction of the AES result can be done by assuming the contributions from one surface layer (having a Mn:Ga ratio of 3:1) and four bulk layers (with 1:1 stoichiometry). The resulting value of such an estimate, assuming an exponential diminishing of the contributions, is found to be 1.8 ± 0.1. This number is within two standard deviations from the measured AES value.

Resolving of these two seemingly conflicting results, namely a higher-than-expected Mn concentration in the surface as well as a lower-than-expected Mn concentration in the bulk, leads to the following emerging conclusion. Evidently, MnGa growth proceeds with preferential Mn segregation to the surface. Slightly Mn-rich flux conditions lead to very Mn-rich surfaces, while simultaneously less Mn incorporates into the bulk. In order to achieve a stoichiometric film, it may thus be necessary to grow under slightly Mn-rich conditions, with the added advantage that the lower surface energy leads to very smooth growth. Future work looking with STM at surface quality as a function of varied flux conditions and film thicknesses could provide further insights into how Mn atoms incorporate into the surface/bulk.

To summarize, this Letter has presented new results based primarily on STM imaging together with theoretical calculations on the MnGa (111) surface grown by MBE. It is found that the growth surface is highly epitaxial with a clear step/terrace structure. The surface reconstruction is mixed with a large portion being 2×2 and relatively smaller fractions having 1×2 or other more complex structures (such as 2×3). Theory calculation finds very good agreement between the STM images and the simulations with Ga atoms dominating

the images for both the 2×2 and 1×2 reconstructions. This study highlights the important relationship between surface and bulk, and further studies in the future will undoubtedly allow even better control of, for example, magnetic properties by careful control of surface structure.

Research supported by the U.S. Department of Energy, Office of Basic Energy Sciences, Division of Materials Sciences and Engineering under Award # DE-FG02-06ER46317. The authors acknowledge the WSxM software for image processing.[16] N. T. thanks DGAPA project IN103512-3 and Conacyt Project 164485 for partial financial support. Calculations were performed in the DGCTIC-UNAM supercomputing center as well as in the Ohio Supercomputer Center, Glenn cluster.

[1] T. J. Nummy, S. P. Bennett, T. Cardinal, and D. Heiman, Appl. Phys. Lett. **99**, 252506 (2011).

[2] S. Mizukami, T. Kubota, F. Wu, X. Zhang, T. Miyazaki, H. Naganuma, M. Oogane, A. Sakuma, and Y. Ando, Phys. Rev. B **85**, 014416 (2012).

[3] T. Saito and R. Nishimura, J. Appl. Phys. **112**, 083901 (2012).

[4] K. K. Wang, E. Lu, J. W. Knepper, F. Y. Yang, and A. R. Smith, Appl. Phys. Lett. **98**, 162507 (2011).

[5] T. Graf, C. Felser and S. Parker, Prog. Solid State Chem. **39**, 1 (2011).

[6] X.Y. Dong, J.W. Dong, J.Q. Xie, T.C. Shih, S. McKernan, C. Leighton and C.J. Palmstrom, J. Cryst. Growth **254**, 384 (2003).

[7] A. Bedoya-Pinto, C. Zube, J. Malindretos, A. Urban and A. Rizzi, Phys. Rev. B **84**, 104424 (2011).

[8] E. Lu, D. C. Ingram, A. R. Smith, J. W. Knepper and F. Y. Yang, Phys. Rev. Lett. **97**, 146101 (2006).

[9] V. P. LaBella, M. R. Krause, Z. Ding, and P. M. Thibado, Surf. Sci. Rep. **60**, 1 (2005).

[10] P. Giannozzi, S. Baroni, N. Bonini, M. Calandra, R. Car, C. Cavazzoni, D. Ceresoli, G. L. Chiarotti, M. Cococcioni, I. Dabo, A. Dal Corso, S. Fabris, G. Fratesi, S. de Gironcoli, R. Gebauer, U. Gerstmann, C. Gougoussis, A. Kokalj, M. Lazzeri, L. Martin-Samos, N. Marzari, F. Mauri, R. Mazzarello, S. Paolini, A. Pasquarello, L. Paulatto, C. Sbraccia, S. Scandolo, G. Sclauzero, A. P. Seitsonen, A. Smogunov, P. Umari, and R. M. Wentzcovitch, J.Phys.: Condens. Matter. **21**, 395502 (2009).

[11] J.P. Perdew, K. Burke, and M. Ernzerhof, Phys. Rev. Lett. **77**, 3865 (1996).

[12] K. Laasonen, A. Pasquarello, R. Car, C. Lee, and D. Vanderbilt, Phys. Rev. B **77**, 10142 (1993).

[13] J. Tersoff and D. R. Hamman, Phys. Rev. Lett. **50**, 1998 (1983).

[14] H. Niida, T. Hori, H. Onodera, Y. Yamaguchi, and Y. Nakagawa, J. Appl. Phys. **79**, 5946 (1996).

[15] A. Sakuma, J. Magn. Magn. Mater. **187**, 105 (1998).

[16] I. Horcas, R. Fernandez, J. M. Gomez-Rodriguez, J. Colchero, J. Gomez-Herrero and A. M.

Baro, Rev. Sci. Instrum. **78**, 013705 (2007).

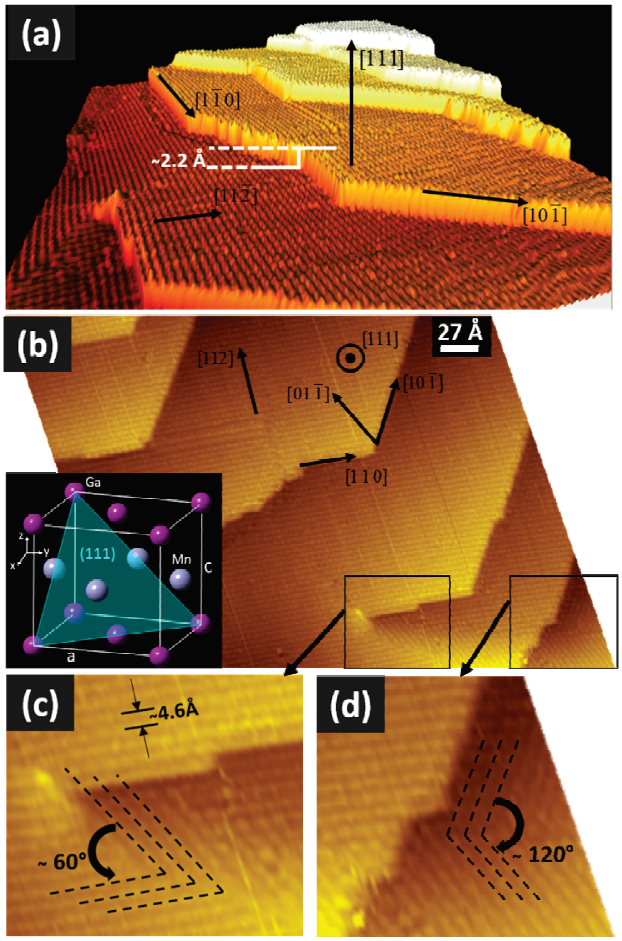

FIG. 1: (a) 3D rendered image of the single atomic steps observed in the MnGa epitaxial structure. (b) Normal plan view STM image of the MnGa structure shown in (a) after drift correction. The inset shows the face centered tetragonal structure of MnGa. Scanning parameters: V_s= -11.0 mV and I_t= 279 pA. (c) and (d) Zoom-in views corresponding to the rectangular boxed areas indicated in (b) showing different domains which come together at ∼60° and ∼120°, respectively.

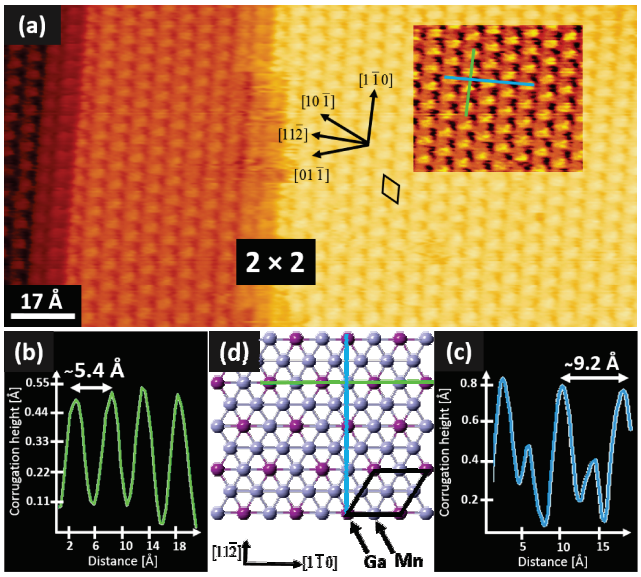

FIG. 2: (a) STM image taken on another area of the same sample, showing a 2×2 (hexagonal-like) surface reconstruction of MnGa; a piece of the upper (bright) terrace was adjusted for contrast, and line profiles were taken along the green and blue path lines. Scanning parameters: V_s= -12.3 mV and I_t= 402 pA. A simple flattening was applied to the image. (b) and (c) Line profiles along the paths shown in (a). (d) Theoretical model for the 2×2 reconstruction, showing the paths (green and blue lines) corresponding to the line profile paths in (a).

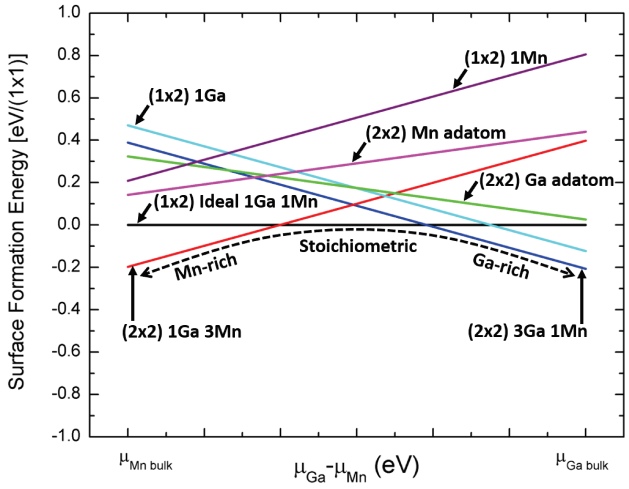

FIG. 3: Total energy plot for various MnGa surface structure models ranging from a Mn-rich 2×2 (1Ga 3Mn) to the ideal stoichiometric 1×2 (1Ga 1Mn) to a Ga-rich 2×2 (3Ga 1Mn). Also included are both vacancy (1Ga, 1Mn) and Ga/Mn adatom models for 1×2 and 2×2 structures, respectively.

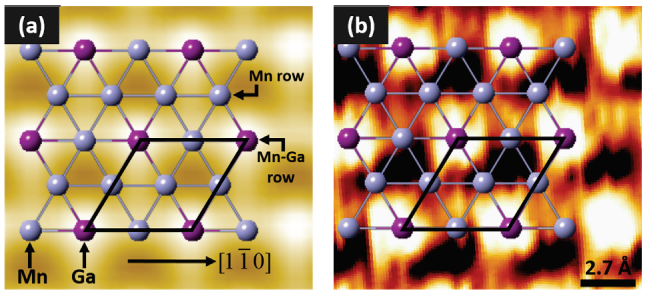

FIG. 4: Simulated and experimental STM images for the Mn-rich 2×2 reconstruction. The theoretical model from Fig. 2(d) was overlaid on both images. The simulation in (a) corresponds to the bias voltage of -12.3 mV for the experimental STM image in (b). STM tunneling current is I_t = 402 pA.

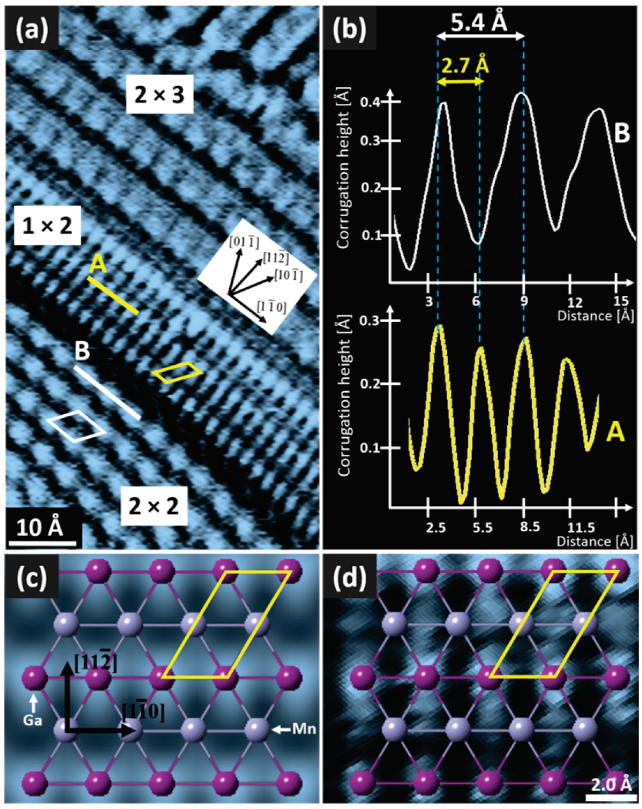

FIG. 5: (a) STM image taken on a different region of the same sample. Three different reconstructions are observed: a 2×2 (lower left corner), a row-like 1×2 (center region), and a more complex one in the remaining space. Scanning parameters: V_s= -6.2 mV and I_t= 293 pA. (b) Line profiles for the 1×2 (A) and 2×2 (B) showing the double spacing of the 2×2 as compared to the 1×2. (c) and (d) Simulated and experimental STM images [zoomed from (a)] for the 1×2, corresponding to the bias voltage V_s= -6.2 mV. The theoretical model for the 1×2 was overlaid on both images.

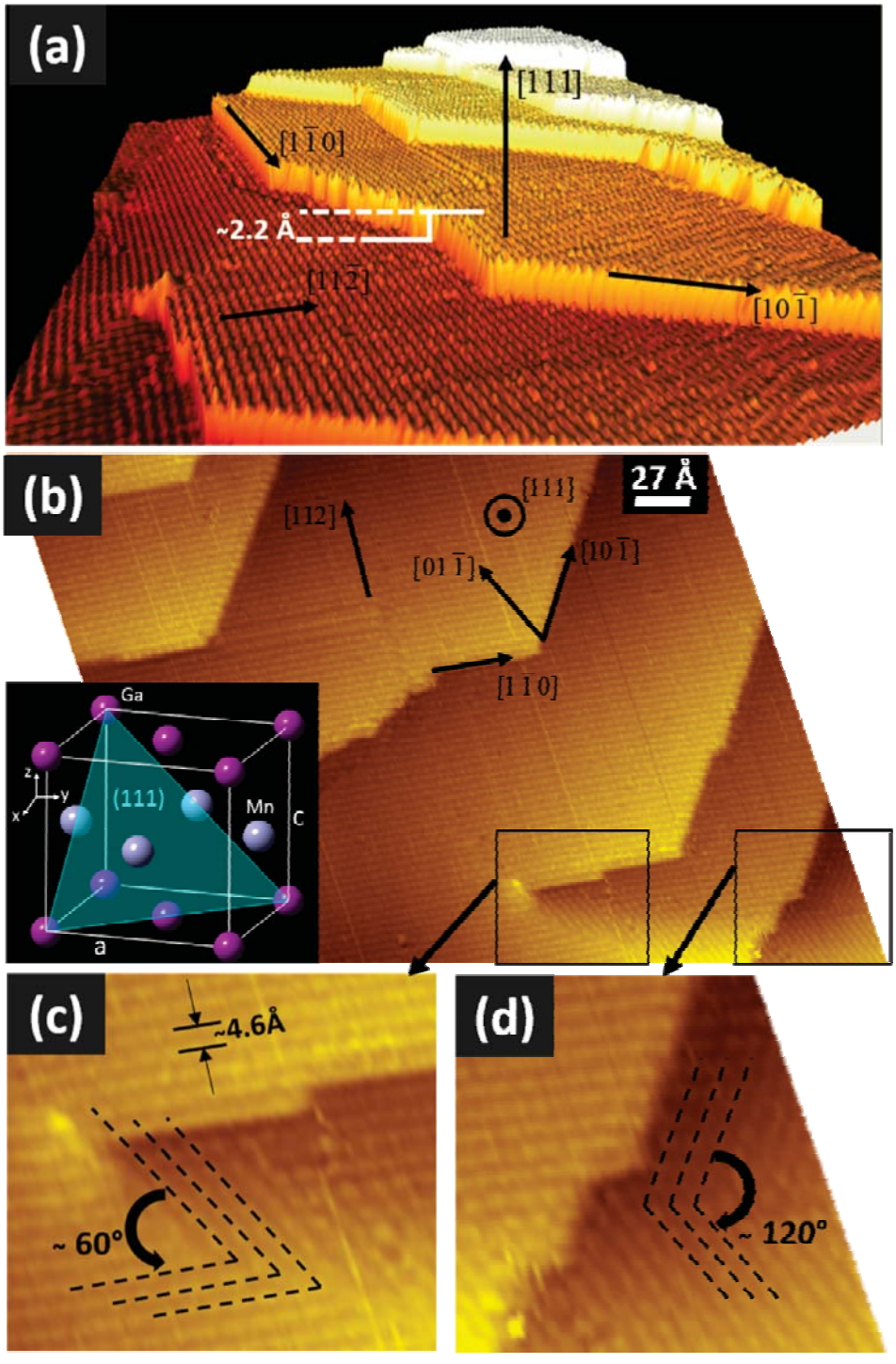
(a)
[1 1 1]
[1 $\bar{1}$ 0]
~2.2 Å
[1 1 $\bar{2}$]
[10 $\bar{1}$]
(b)
27 Å
[112]
[111]
[01 $\bar{1}$]
[10 $\bar{1}$]
[1 1 0]
Ga
(111)
Mn
c
a
z
y
x
(c)
~4.6Å
~ 60°
(d)
~ 120°

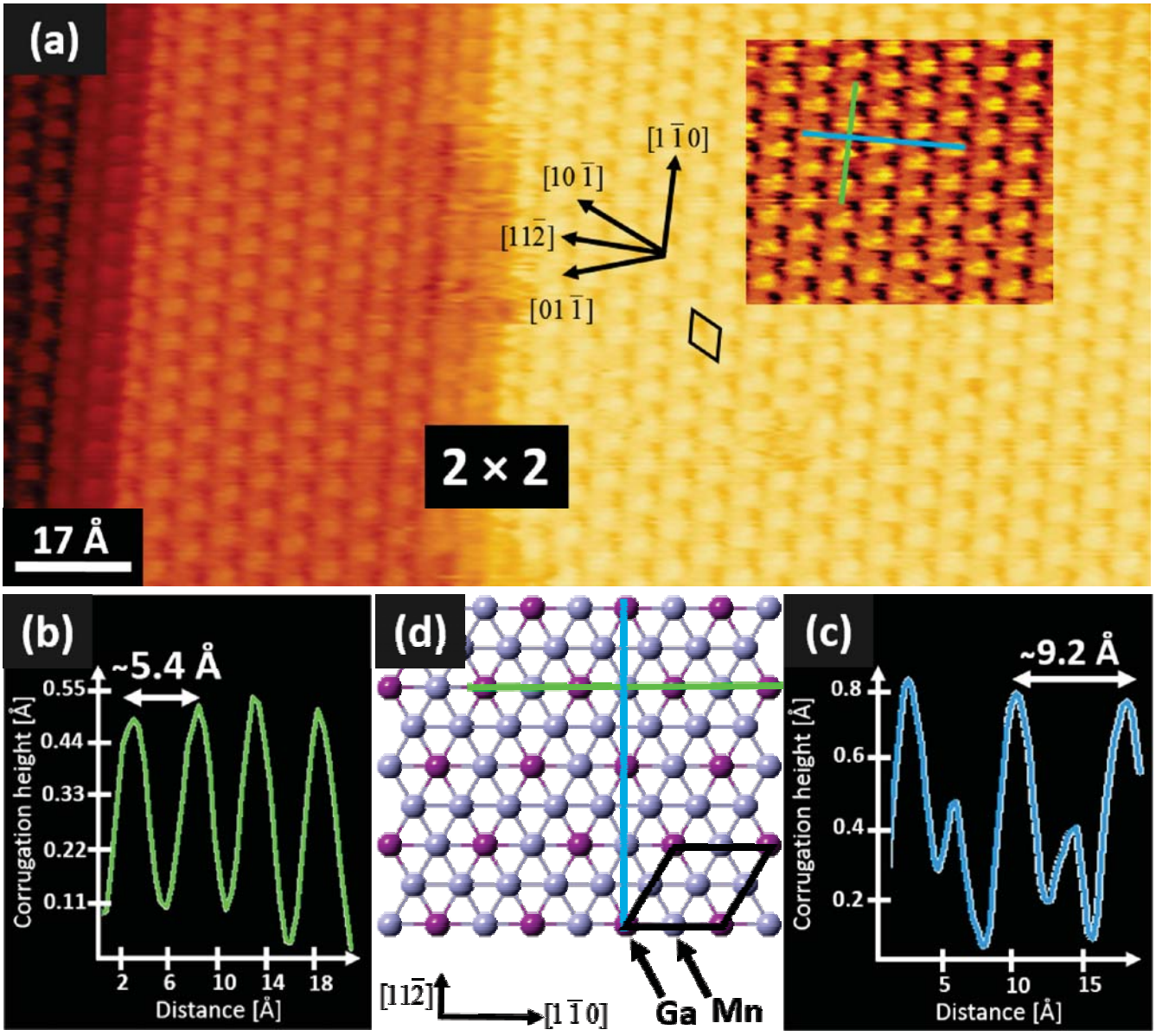
(a)
[1 $\bar{1}$ 0]
[10 $\bar{1}$]
[11$\bar{2}$]
[01 $\bar{1}$]
2 × 2
17 Å
(b)
~5.4 Å
Corrugation height [Å]
0.55
0.44
0.33
0.22
0.11
2
6
10
14
18
Distance [Å]
(d)
[11$\bar{2}$]
[1 $\bar{1}$ 0]
Ga
Mn
(c)
~9.2 Å
Corrugation height [Å]
0.8
0.6
0.4
0.2
5
10
15
Distance [Å]

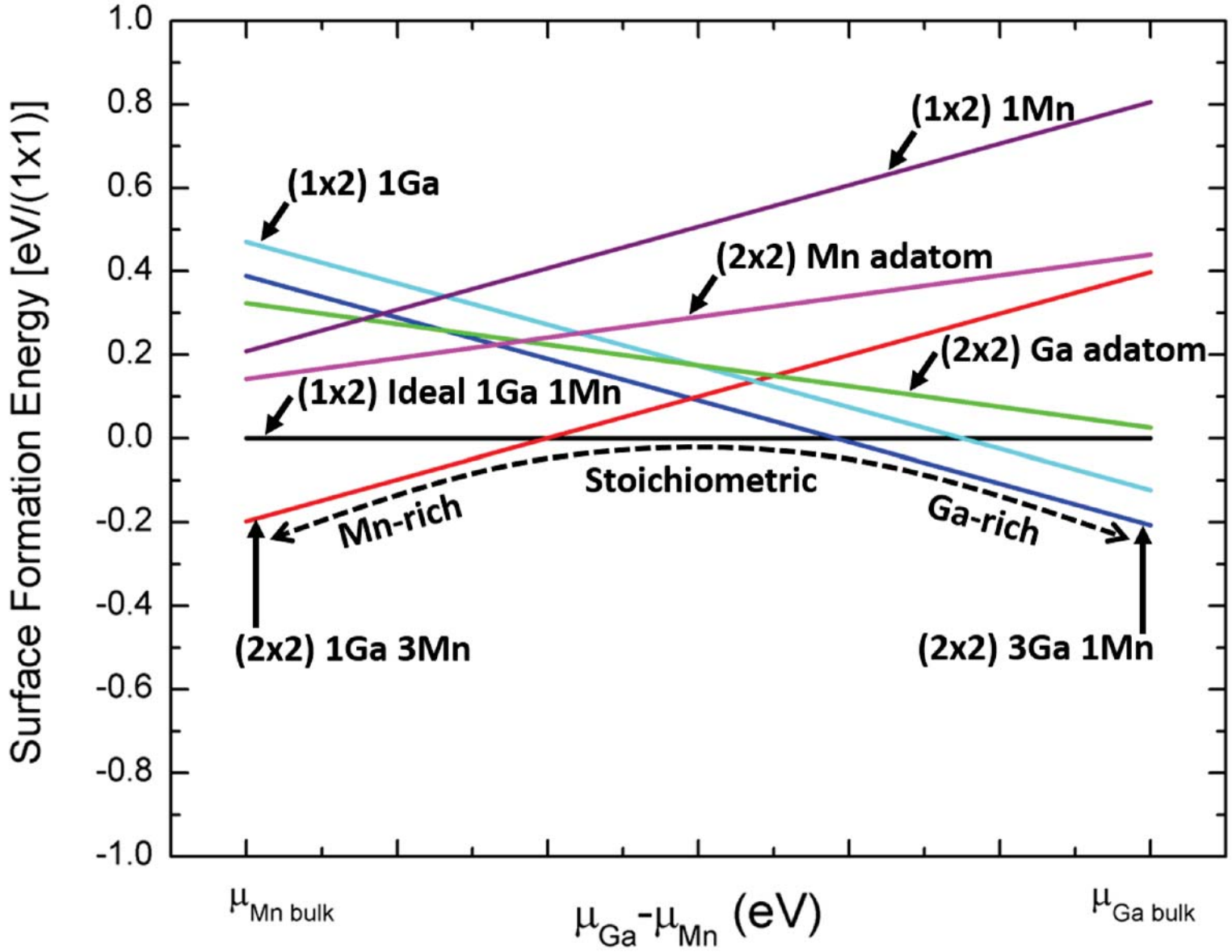
Surface Formation Energy [eV/(1x1)]
1.0
0.8
0.6
0.4
0.2
0.0
-0.2
-0.4
-0.6
-0.8
-1.0
(1x2) 1Mn
(1x2) 1Ga
(2x2) Mn adatom
(2x2) Ga adatom
(1x2) Ideal 1Ga 1Mn
Stoichiometric
Mn-rich
Ga-rich
(2x2) 1Ga 3Mn
(2x2) 3Ga 1Mn
μMn bulk
μGa-μMn (eV)
μGa bulk

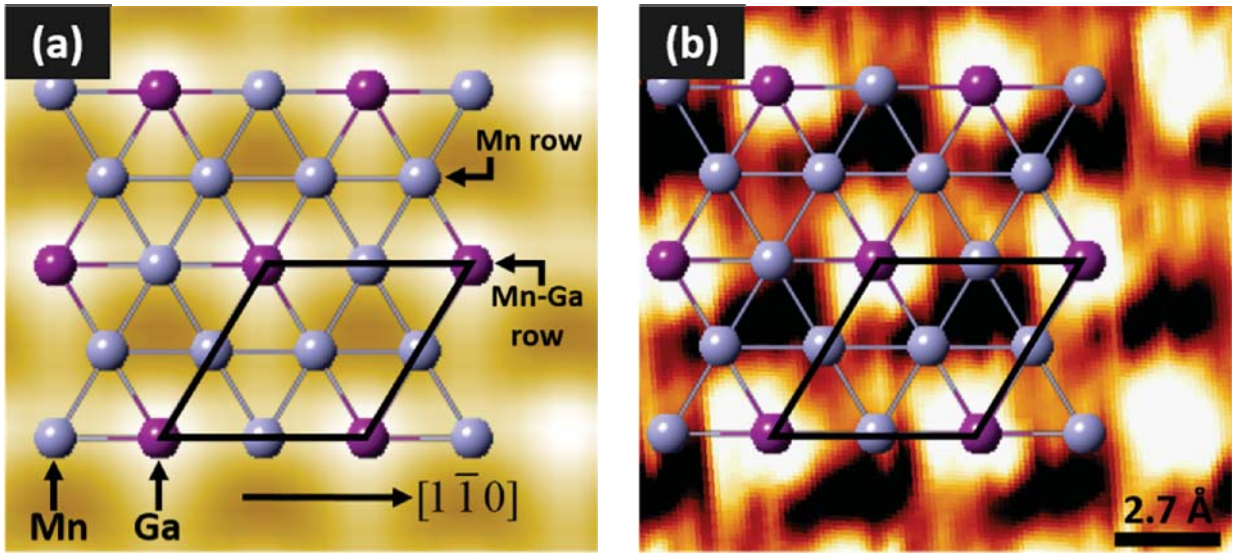
(a)
Mn row
Mn-Ga
row
Mn
Ga
[1 $\bar{1}$ 0]
(b)
2.7 Å

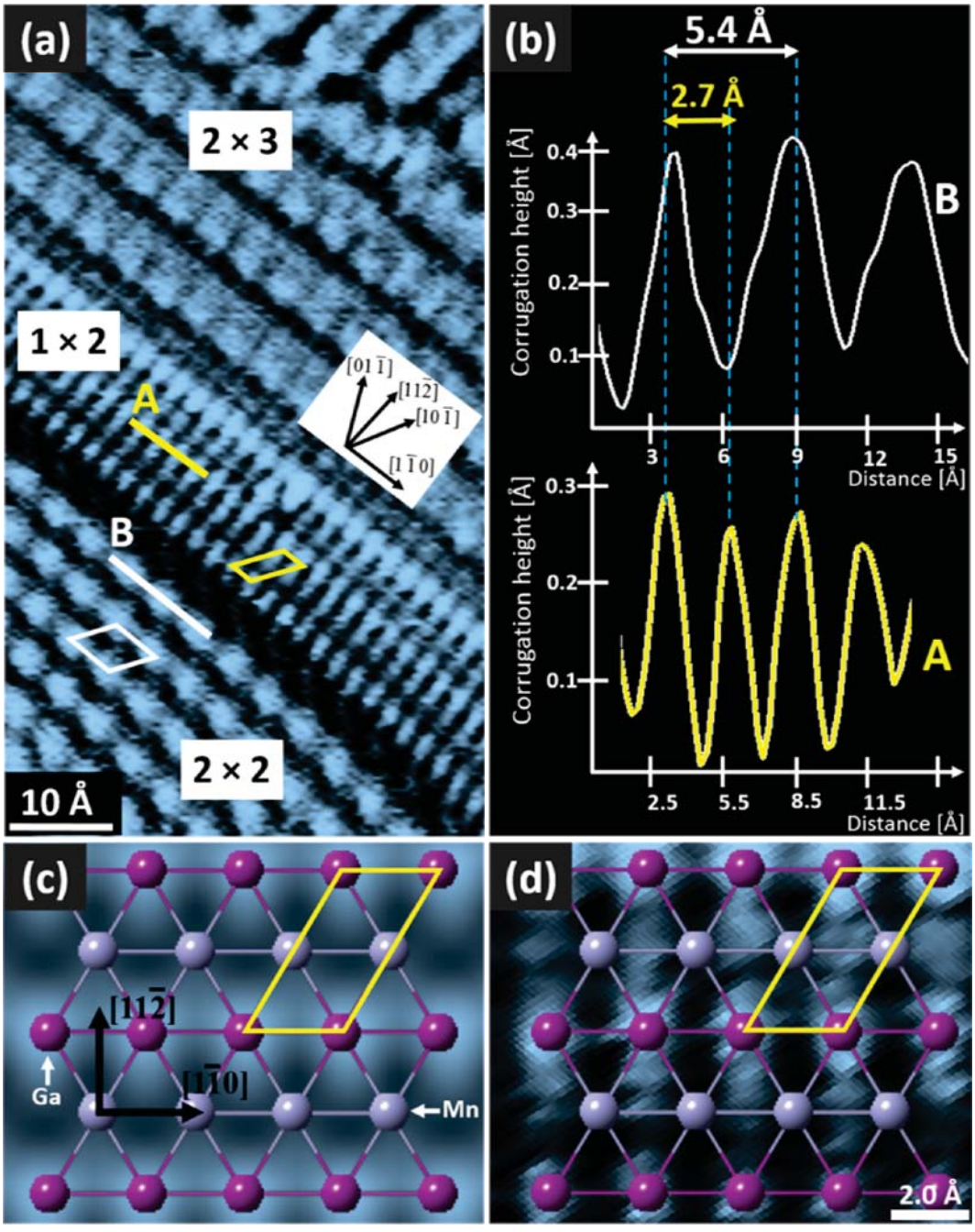
(a)
2 × 3
1 × 2
2 × 2
A
B
10 Å
[0 1 $\bar{1}$]
[1 1 $\bar{2}$]
[1 0 $\bar{1}$]
[1 $\bar{1}$ 0]
(b)
5.4 Å
2.7 Å
Corrugation height [Å]
0.4
0.3
0.2
0.1
B
3
6
9
12
15
Distance [Å]
0.3
0.2
0.1
A
2.5
5.5
8.5
11.5
Distance [Å]
(c)
[1 1 $\bar{2}$]
[1 $\bar{1}$ 0]
Ga
Mn
(d)
2.0 Å